

Asymmetries in ϕ photoproduction and the Okubo-Zweig-Iizuka violation

Yongseok Oh^{a*} and H. C. Bhang^b

^a *Institute of Physics and Applied Physics, Department of Physics, Yonsei University, Seoul 120-749, Korea*

^b *Department of Physics, Seoul National University, Seoul 151-742, Korea*

Abstract

We study the vector meson density matrix and the associated polarization asymmetries in ϕ photoproduction near threshold. In order to study the OZI violating processes, we consider the direct ϕNN coupling as well as the knockout processes arising from the non-vanishing $s\bar{s}$ sea quarks in the nucleon. The polarization asymmetries in ϕ meson decays are found to be very useful to constrain the ϕNN coupling constant. The hidden strangeness of the nucleon can also be studied by these asymmetries, but mostly at large $|t|$ region.

13.88.+e, 13.25.Gv, 13.60.Le, 24.70.+s

Typeset using REVTeX

*E-mail address : yoh@phya.yonsei.ac.kr

The electromagnetic production of ϕ meson from the nucleon has been suggested as a sensitive probe to study the hidden strangeness of the nucleon [1–6]. This is because the ϕ is nearly pure $s\bar{s}$ state so that its direct coupling to the nucleon is suppressed by the OZI rule. However, if there exists a non-vanishing $s\bar{s}$ sea quark component in the nucleon, the strange sea quarks can contribute to the ϕ production via the OZI evasion processes. Investigation of such processes can then be expected to shed light on the nucleon strangeness content, if any [7,8].

In a series of publication, it has been argued that the double polarization asymmetries of ϕ photo- and electroproduction from the nucleon targets at threshold energy region can be used to probe the hidden strangeness content of the nucleon [4–6]. In addition to the direct knockout production mechanisms, the direct ϕNN coupling can also induce an OZI evading process [9–11]. Even if we assume the ideal mixing of the ϕ with the ω , the effective ϕNN coupling is allowed by the kaon loops and hyperon excitations. But the smallness of the effective ϕNN coupling constants estimated by this approach reveals the validity of the OZI rule [12]. However the analyses of electromagnetic nucleon form factors [13–15] and the baryon-baryon scattering [16–18] suggest strongly a fairly large ϕNN vector coupling constant which violates the OZI rule. The recent CLAS experiments on ϕ photoproduction at large momentum transfers [19], therefore, open another way to constrain the ϕNN coupling. The data show increasing differential cross sections at large $|t|$, which has been interpreted as the contributions from the u -channel nucleon exchanges [20]. It has been recently re-analysed to probe the nucleon resonances which couple to the ϕN channel in an SU(3) quark model [21,22]. The recent CLAS data on ϕ photo- and electroproduction [19,23] also lead to a discussion on the role of the axial ghost pole in vector meson electromagnetic production at low energies and large momentum transfers [24].

In this paper, we re-analyse the CLAS data by extending the work of Refs. [4,5]. As the production models, we consider the Pomeron exchange, π and η exchange, nucleon pole terms with adjustable ϕNN couplings, and the direct knockouts. We study the vector meson density matrix and the associated polarization asymmetries in ϕ photoproduction and find that they are useful to investigate the ϕNN coupling as well as the knockout mechanisms.

We start with defining the kinematic variables. The four-momenta of the incoming photon, outgoing ϕ meson, and initial/final proton are denoted by k , q , p , and p' , respectively. The Mandelstam variables are defined as $W^2 = (p + k)^2$ and $t = (p - p')^2$. The photon laboratory energy is denoted by E_γ . We assume that the production amplitudes include the Pomeron exchange [Fig. 1(a)] and the pseudoscalar-meson (π, η) exchange [Fig. 1(b)]. With the above t -channel background processes we study the direct and crossed nucleon pole terms [Fig. 1(c,d)] as well as the direct knockout mechanisms [Fig. 1(e,f)].

For the Pomeron exchange, which governs the total cross sections and differential cross sections at low $|t|$, we follow the Donnachie-Landshoff model [25–28], which gives [29,30]

$$T_{fi}^P = iM_0(s, t) \bar{u}_{m_f}(p') \varepsilon_\mu^*(\phi) \{k^\mu g^{\mu\nu} - k^\nu \gamma^\mu\} \varepsilon_\nu(\gamma) u_{m_i}(p), \quad (1)$$

where $\varepsilon_\mu(\phi)$ and $\varepsilon_\nu(\gamma)$ are the polarization vectors of the ϕ meson and photon, respectively, and $u_m(p)$ is the Dirac spinor of the nucleon with momentum p and spin projection m . The Pomeron exchange is described by the following Regge parameterization:

$$M_0(s, t) = C_V F_1(t) F_V(t) \left(\frac{s}{s_0} \right)^{\alpha_P(t)-1} \exp \left\{ -\frac{i\pi}{2} [\alpha_P(t) - 1] \right\}, \quad (2)$$

where $F_1(t)$ is the isoscalar electromagnetic form factor of the nucleon and $F_V(t)$ is the form factor for the vector-meson-photon-Pomeron coupling:

$$F_1(t) = \frac{4M_N^2 - 2.8t}{(4M_N^2 - t)(1 - t/t_0)^2}, \quad F_V(t) = \frac{1}{1 - t/M_V^2} \frac{2\mu_0^2}{2\mu_0^2 + M_V^2 - t}, \quad (3)$$

where $t_0 = 0.7 \text{ GeV}^2$ and M_N (M_V) is the nucleon (ϕ meson) mass. The Pomeron trajectory is known to be $\alpha_P(t) = 1.08 + 0.25t$. The strength factor C_V reads $C_V = 12\sqrt{4\pi\alpha_{\text{em}}}\beta_0\beta_s/f_V$ with the vector meson decay constant f_V ($= 13.13$ for the ϕ meson) and $\alpha_{\text{em}} = e^2/4\pi$. By fitting all of the total cross section data for ω , ρ , and ϕ photoproduction at high energies, the remaining parameters of the model are determined: $\mu_0^2 = 1.1 \text{ GeV}^2$, $\beta_0 = 2.05 \text{ GeV}^{-1}$, $\beta_s = 1.60 \text{ GeV}^{-1}$, and $s_0 = 4 \text{ GeV}^2$.

The pseudoscalar-meson exchange is known to be an important correction to the Pomeron exchange at low energies. The amplitude can be calculated from the following effective Lagrangians,

$$\begin{aligned} \mathcal{L}_{\phi\gamma\Pi} &= \frac{eg_{\phi\gamma\Pi}}{M_V} \epsilon^{\mu\nu\alpha\beta} \partial_\mu \phi_\nu \partial_\alpha A_\beta \Pi, \\ \mathcal{L}_{\Pi NN} &= \frac{g_{\pi NN}}{2M_N} \bar{N} \gamma^\mu \gamma_5 \tau_3 N \partial_\mu \pi^0 + \frac{g_{\eta NN}}{2M_N} \bar{N} \gamma^\mu \gamma_5 N \partial_\mu \eta, \end{aligned} \quad (4)$$

where $\Pi = (\pi^0, \eta)$ and A_β is the photon field. The resulting invariant amplitude reads

$$T_{fi}^{ps} = \sum_{\Pi=\pi,\eta} \frac{-iF_{\Pi NN}(t)F_{\phi\gamma\Pi}(t)}{t - M_\Pi^2} \frac{eg_{\phi\gamma\Pi}g_{\Pi NN}}{M_V} \bar{u}_{m_f}(p') \gamma_5 u_{m_i}(p) \epsilon^{\mu\nu\alpha\beta} q_\mu k_\alpha \epsilon_\nu^*(\phi) \epsilon_\beta(\gamma). \quad (5)$$

In the above, we have followed Ref. [31] to include the form factors to dress the ΠNN and $\phi\gamma\Pi$ vertices as

$$F_{\Pi NN}(t) = \frac{\Lambda_\Pi^2 - M_\Pi^2}{\Lambda_\Pi^2 - t}, \quad F_{\phi\gamma\Pi}(t) = \frac{\Lambda_{\phi\gamma\Pi}^2 - M_\Pi^2}{\Lambda_{\phi\gamma\Pi}^2 - t}. \quad (6)$$

We use $g_{\pi NN}^2/4\pi = 14$ for the πNN coupling constant. The ηNN coupling constant is not well determined [32]. In the case of ω photoproduction, the higher mass of the η and the smallness of the $\omega\gamma\eta$ coupling constant suppress the contribution of the η exchange compared with that of the π exchange [33]. However in the case of ϕ photoproduction, the η exchange contribution may be larger than the π exchange at large $|t|$ depending on the ηNN coupling constant because of the large value of the $\phi\gamma\eta$ coupling. The dependence of the cross sections on $g_{\eta NN}$ was discussed in detail by Ref. [11] and in this study we use $g_{\eta NN}^2/4\pi = 0.99$ which is obtained from making use of the SU(3) symmetry relation together with a recent value of $F/D = 0.575$. The coupling constants $g_{\phi\gamma\Pi}$ can be estimated through the decay widths of $\phi \rightarrow \gamma\pi$ and $\phi \rightarrow \gamma\eta$ [34], which lead to $g_{\phi\gamma\pi} = 0.14$ and $g_{\phi\gamma\eta} = 0.704$. The amplitudes are also dependent of the cutoff parameters Λ_Π and $\Lambda_{\phi\gamma\Pi}$ in Eq. (6), which

are fitted by the experimental data [19,35] at small and medium $|t|$ region and from Ref. [11]: $\Lambda_\pi = 0.9$ GeV, $\Lambda_{\phi\gamma\pi} = 0.9$ GeV, $\Lambda_\eta = 1.0$ GeV and $\Lambda_{\phi\gamma\eta} = 0.9$ GeV.

We evaluate the nucleon pole terms shown in Fig. 1(c,d) from the following interaction Lagrangians,

$$\begin{aligned}\mathcal{L}_{\gamma NN} &= -e\bar{N} \left(\gamma_\mu \frac{1 + \tau_3}{2} A^\mu - \frac{\kappa_N}{2M_N} \sigma^{\mu\nu} \partial_\nu A_\mu \right) N, \\ \mathcal{L}_{\phi NN} &= -g_{\phi NN} \bar{N} \left(\gamma_\mu \phi^\mu - \frac{\kappa_\phi}{2M_N} \sigma^{\mu\nu} \partial_\nu \phi_\mu \right) N,\end{aligned}\quad (7)$$

with the anomalous magnetic moment of the nucleon $\kappa_{p(n)} = 1.79$ (-1.91). There are big uncertainties with the ϕNN coupling constants. First, the effective ϕNN coupling through kaon loops and hyperon excitations was estimated to be very small, $g_{\phi NN} \simeq -0.24$ [12], which is consistent with the OZI rule prediction. However the analyses on the electromagnetic nucleon form factors [13–15] and the baryon-baryon scattering [16–18] favor a large ϕNN vector coupling constant which strongly violates the OZI rule: $g_{\phi NN}/g_{\omega NN} = -0.3 \sim -0.43$, therefore $g_{\phi NN} = -2.3 \sim -4.7$ with $g_{\omega NN} = 7.0 \sim 11.0$ [36]. In our study the nucleon pole terms are responsible to the recent CLAS data on ϕ photoproduction at large $|t|$ and we fit the data with the $g_{\phi NN}$ and find that $|g_{\phi NN}| = 3.0$ can reproduce the data, which is consistent with the Regge trajectory study of Ref. [20]. The tensor coupling constant κ_ϕ has been estimated to be $\kappa_\phi/\kappa_\omega = 0.5 \sim 2.1$ [15,16] or $\kappa_\phi \simeq \pm 0.2$ [12]. However, it is known that the value of the tensor coupling κ_ω is very small as discussed in a study of πN scattering and pion photoproduction [36]. Thus we use $\kappa_\phi = 0$ in our calculation. We also found that the results are not dependent on κ_ϕ if $\kappa_\phi < 1$. The resulting invariant amplitude reads

$$T_{fi}^N = \bar{u}_{m_f}(p') \varepsilon^{\mu*}(\phi) M_{\mu\nu} \varepsilon^\nu(\gamma) u_{m_i}(p), \quad (8)$$

where

$$M_{\mu\nu} = -e g_{\phi NN} \left[\Gamma_\mu^\phi(q) \frac{\not{p} + \not{k} + M_N}{s - M_N^2} \Gamma_\nu^\gamma(k) F_N(s) + \Gamma_\nu^\gamma(k) \frac{\not{p}' - \not{q} + M_N}{u - M_N^2} \Gamma_\mu^\phi(q) F_N(u) \right] \quad (9)$$

with

$$\Gamma_\mu^\phi(q) = \gamma_\mu - i \frac{\kappa_\phi}{2M_N} \sigma_{\mu\alpha} q^\alpha, \quad \Gamma_\nu^\gamma(k) = \gamma_\nu + i \frac{\kappa_p}{2M_N} \sigma_{\nu\beta} k^\beta, \quad (10)$$

and $s = (p + k)^2$, $u = (p - q)^2$. Here we follow Ref. [37] to include a form factor

$$F_N(r) = \frac{\Lambda_N^4}{\Lambda_N^4 - (r - M_N^2)^2} \quad (11)$$

with $r = s$ or t . The gauge invariance is restored by projecting out the gauge non-invariant parts [33] and we use the cutoff parameter $\Lambda_N = 0.5$ GeV as in the study of ω photoproduction [33].

If we assume a non-vanishing strange sea quarks in the nucleon wavefunction, it can contribute to ϕ photoproduction through direct knockout mechanisms [2] [Fig. 1(e,f)].¹ In order to investigate the effects from the hidden strangeness content of the proton in ϕ photoproduction, we parameterize the proton wavefunction in Fock space as

$$|p\rangle = A_0|uud\rangle + \sum_X A_X|uudX\rangle + \sum_X B_X|uuds\bar{s}X\rangle, \quad (12)$$

where X denotes any combination of gluons and light quark pairs of u and d quarks. Ellis *et al.* [38] estimated it to be 1–19% from an analysis of $p\bar{p}$ annihilation. From the ϕ electroproduction process, Henley *et al.* [2] claimed that its theoretical upper-bound would be 10–20%. By employing a relativistic quark model [3] it was shown that the upper-bound could be lowered to 3–5%. For simplicity and for our qualitative study, we approximate the proton wavefunction (12) as

$$\begin{aligned} |p\rangle &= A|uud\rangle + B|uuds\bar{s}\rangle \\ &= A[|uud\rangle]^{1/2} + \sum_{j_{s\bar{s}}=0,1;j_c} b_{j_{s\bar{s}}} |[[|uud\rangle]^{1/2} \otimes [\mathbf{L}]^{j_c} \otimes [s\bar{s}]^{j_{s\bar{s}}}]^{1/2}\rangle, \end{aligned} \quad (13)$$

where \mathbf{L} is the relative angular momentum of the two clusters. This parameterization of the nucleon wavefunction can be justified in ϕ production as argued in Refs. [2,3]. The strangeness content B^2 should be determined by further theoretical and experimental studies and we present our results with varying this value. The production amplitude of this mechanism has been discussed extensively in Refs. [3,5] and will not be repeated here.

Within the models discussed above, we present the differential cross sections of ϕ photoproduction at $E_\gamma = 2.0$ GeV and 3.6 GeV in Fig. 2. In the considered energy region, it can be seen that the Pomeron exchange (dashed lines) gives the dominant contribution at small $|t|$ region. The pseudoscalar-meson exchange (dotted line) is important at medium $|t|$ region while the nucleon pole terms are responsible for the increase of the differential cross sections at large $|t|$. With $|g_{\phi NN}| = 3.0$, we could reproduce the recent CLAS data on ϕ photoproduction [19]. This is consistent with the results of Ref. [20] based on Regge trajectory. The direct knockout mechanism is suppressed and thus cannot be distinguished from the other mechanisms unless we study other quantities such as the polarization asymmetries [4,5].

Although the analyses on electromagnetic nucleon form factor and baryon-baryon scattering supports the large value of the ϕNN coupling, one can further constrain the coupling in ϕ photoproduction. The electromagnetic nucleon form factor study based on vector meson dominance only tells that the relative phase between the $\phi\gamma$ coupling and the ϕNN coupling is negative. We found that the asymmetries in ϕ photoproduction can give us a clue on the phase of the ϕNN coupling and therefore the vector meson dominance in electromagnetic

¹The direct knockout mechanisms may be related to the loop diagrams of the effective ϕNN vertex considered in Ref. [12], i.e., the meson clouds of the nucleon or the intermediate baryons may interact with the photon to produce the ϕ meson. Since we are considering tree diagrams only, however, clarifying that issue is beyond the scope of this work.

nucleon form factor can be tested directly. (In our convention, the $\phi\gamma$ coupling has positive sign.) For this purpose, we compute the ϕ meson density matrix elements within our model. The results at $E_\gamma = 2.8$ GeV in *helicity frame* [39] are shown in Fig. 3. The solid lines are obtained with $g_{\phi NN} = -3.0$ while the dashed lines are with $g_{\phi NN} = +3.0$. The contributions from the direct knockout mechanisms are small and cannot be seen here. Figure 3 shows that the vector meson density matrix is strongly dependent on the phase of the $g_{\phi NN}$ at large $|t|$.

This difference can be readily seen in the photon polarization asymmetry Σ_ϕ and the parity asymmetry P_σ which are defined as

$$\begin{aligned}\Sigma_\phi &\equiv \frac{\sigma_{\parallel} - \sigma_{\perp}}{\sigma_{\parallel} + \sigma_{\perp}} = \frac{1}{p_\gamma} \frac{W^L(0, \frac{\pi}{2}, \frac{\pi}{2}) - W^L(0, \frac{\pi}{2}, 0)}{W^L(0, \frac{\pi}{2}, \frac{\pi}{2}) + W^L(0, \frac{\pi}{2}, 0)}, \\ P_\sigma &\equiv \frac{\sigma^N - \sigma^U}{\sigma^N + \sigma^U} = 2\rho_{1-1}^1 - \rho_{00}^1,\end{aligned}\tag{14}$$

where W^L is the decay angular distribution of the ϕ meson, σ_{\parallel} (σ_{\perp}) is the cross sections for symmetric decay particle pairs produced parallel (normal) to the photon polarization plane and σ^N (σ^U) is the contribution of natural (unnatural) parity exchanges to the cross section. The details on the definitions and physical meanings of those asymmetries can be found, e.g., in Refs. [39,40]. Shown in Fig. 4 are our results for the asymmetries at $E_\gamma = 3.6$ GeV. As can be seen in Fig. 4, measuring those asymmetries can be used to constrain the ϕNN coupling and can test the vector meson dominance hypothesis.

As discussed in Refs. [4,5] and can be verified from Fig. 2, however, the direct knockout mechanisms could be investigated only at lower energies, i.e., near the threshold. Therefore, we compute the polarization asymmetries at $E_\gamma = 2.0$ GeV in Fig. 5. The dashed lines are obtained without the knockout mechanisms, i.e., with $B^2 = 0$, while the solid and dot-dashed lines are with $B^2 = 1\%$ and 2% , respectively. The results are dependent on the phases of $b_{0,1}$ and the phases of b_0 and b_1 are assumed to be positive in Fig. 5 for simplicity. We have used $g_{\phi NN} = -3.0$ in the calculation. The difference of the results depending on B^2 can be seen especially at large $|t|$ region. Although the difference is not as large as in Fig. 4, it can be used for to study the uud knockout process [Fig. 1(f)] and might be tested experimentally.

In summary, we have investigated the vector meson density matrix and the associated polarization asymmetries in ϕ photoproduction at low energies. As the models for ϕ photoproduction, we have considered the Pomeron and pseudoscalar (π, η) exchanges, nucleon pole terms, and the direct knockouts. We found that the recent CLAS data on ϕ photoproduction can be explained by a rather large ϕNN coupling, i.e. $g_{\phi NN} = -3.0$, which supports the result of Ref. [20]. This value is larger than the expectations based on the OZI rule, but is consistent with the values estimated in electromagnetic nucleon form factors and baryon-baryon scattering. As another test for constraining $g_{\phi NN}$ we computed the vector meson density matrix and the polarization asymmetries. It was shown that they are strongly dependent on the ϕNN coupling constant. The results are different from the predictions of Ref. [22] which includes the nucleon resonances decaying into ϕN channel within an SU(3) quark model. Thus the polarization asymmetries can be used to test the models for the nucleon pole terms and the nucleon resonances. Finally, we have shown that they can be

used to probe the hidden strangeness content of the nucleon. Those observables could be measured at current experimental facilities such as Thomas Jefferson National Accelerator Facility and LEPS of SPring-8. On the theoretical side, further investigations are needed for clarifying the model dependence of our results and understanding the contributions from the loop diagrams which give an effective ϕNN coupling through the rescattering processes.

ACKNOWLEDGMENTS

We are grateful to V. Burkert, M. Fujiwara, T.-S. H. Lee, and E. Smith for fruitful discussions. This work was supported in part by the Brain Korea 21 project of Korean Ministry of Education and the International Collaboration Program of KOSEF under Grant No. 20006-111-01-2.

REFERENCES

- [1] E. M. Henley, G. Krein, S. J. Pollock, and A. G. Williams, Phys. Lett. B **269**, 31 (1991).
- [2] E. M. Henley, G. Krein, and A. G. Williams, Phys. Lett. B **281**, 178 (1992).
- [3] A. I. Titov, Y. Oh, and S. N. Yang, Chin. J. Phys. (Taipei) **32**, 1351 (1994); A. I. Titov, S. N. Yang, and Y. Oh, Nucl. Phys. **A618**, 259 (1997).
- [4] A. I. Titov, Y. Oh, and S. N. Yang, Phys. Rev. Lett. **79**, 1634 (1997).
- [5] A. I. Titov, Y. Oh, S. N. Yang, and T. Morii, Phys. Rev. C **58**, 2429 (1998).
- [6] Y. Oh, A. I. Titov, S. N. Yang, and T. Morii, Phys. Lett. B **462**, 23 (1999); Nucl. Phys. **A684**, 354 (2001).
- [7] J. Ellis, M. Karliner, D. E. Kharzeev, and M. G. Sapozhnikov, Nucl. Phys. **A673**, 256 (2000).
- [8] J. Ellis, Nucl. Phys. A **684**, 53 (2001).
- [9] R. A. Williams, Phys. Rev. C **57**, 223 (1998).
- [10] A. Titov, T.-S. H. Lee, and H. Toki, Phys. Rev. C **59**, 2993 (1999).
- [11] A. I. Titov, T.-S. H. Lee, H. Toki, and O. Streltsova, Phys. Rev. C **60**, 035205 (1999).
- [12] U.-G. Meißner, V. Mull, J. Speth, and J. W. Van Orden, Phys. Lett. B **408**, 381 (1997).
- [13] H. Genz and G. Höhler, Phys. Lett. **61B**, 389 (1976).
- [14] G. Höhler, E. Pietarinen, I. Sabba-Stefanescu, F. Borkowski, G. G. Simon, V. H. Walther, and R. D. Wendling, Nucl. Phys. **B114**, 505 (1976).
- [15] R. L. Jaffe, Phys. Lett. B **229**, 275 (1989).
- [16] M. M. Nagels, T. A. Rijken, and J. J. de Swart, Phys. Rev. D **12**, 744 (1975).
- [17] M. M. Nagels, T. A. Rijken, and J. J. de Swart, Phys. Rev. D **15**, 2547 (1977).
- [18] M. M. Nagels, T. A. Rijken, and J. J. de Swart, Phys. Rev. D **20**, 1633 (1979).
- [19] CLAS Collaboration, E. Anciant *et al.*, Phys. Rev. Lett. **85**, 4682 (2000).
- [20] J. M. Laget, Phys. Lett. B **489**, 313 (2000).
- [21] Q. Zhao, J.-P. Didelez, M. Guidal, and B. Saghai, Nucl. Phys. **A660**, 323 (1999).
- [22] Q. Zhao, B. Saghai, and J. S. Al-Khalili, Phys. Lett. B **509**, 231 (2001).
- [23] CLAS Collaboration, K. Lukashin *et al.*, Phys. Rev. C **63**, 065205 (2001)
- [24] N. I. Kochelev and V. Vento, Universitat de València-CSIC Report No. FTUV-01-0405 (2001), hep-ph/0104070.
- [25] A. Donnachie and P. V. Landshoff, Nucl. Phys. **B244**, 322 (1984).
- [26] A. Donnachie and P. V. Landshoff, Nucl. Phys. **B267**, 690 (1986).
- [27] A. Donnachie and P. V. Landshoff, Phys. Lett. B **185**, 403 (1987).
- [28] A. Donnachie and P. V. Landshoff, Phys. Lett. B **296**, 227 (1992).
- [29] J.-M. Laget and R. Mendez-Galain, Nucl. Phys. **A581**, 397 (1995).
- [30] M. A. Pichowsky and T.-S. H. Lee, Phys. Rev. D **56**, 1644 (1997).
- [31] B. Friman and M. Soyeur, Nucl. Phys. **A600**, 477 (1996).
- [32] L. Tiator, C. Bennhold, and S. S. Kamalov, Nucl. Phys. **A580**, 455 (1994).
- [33] Y. Oh, A. I. Titov, and T.-S. H. Lee, Phys. Rev. C **63**, 025201 (2001).
- [34] Particle Data Group, D. E. Groom *et al.*, Eur. Phys. J. C **15**, 1 (2000).
- [35] H. J. Besch, G. Hartmann, R. Kose, F. Krautschneider, W. Paul, and U. Trinks, Nucl. Phys. **B70**, 257 (1974).
- [36] T. Sato and T.-S. H. Lee, Phys. Rev. C **54**, 2660 (1996).

- [37] B. C. Pearce and B. K. Jennings, Nucl. Phys. **A528**, 655 (1991); H. Habermehl, C. Bennhold, T. Mart, and T. Feuster, Phys. Rev. C **58**, 40 (1998).
- [38] J. Ellis, M. Karliner, D. E. Kharzeev, and M. G. Sapozhnikov, Phys. Lett. B **353**, 319 (1995).
- [39] K. Schilling, P. Seyboth, and G. Wolf, Nucl. Phys. **B15**, 397 (1970), **B18**, 332(E) (1970).
- [40] J. Ballam *et al.*, Phys. Rev. D **5**, 545 (1972).
- [41] LAMP2 Collaboration, D. P. Barber *et al.*, Phys. Lett. **79B**, 150 (1978).

FIGURES

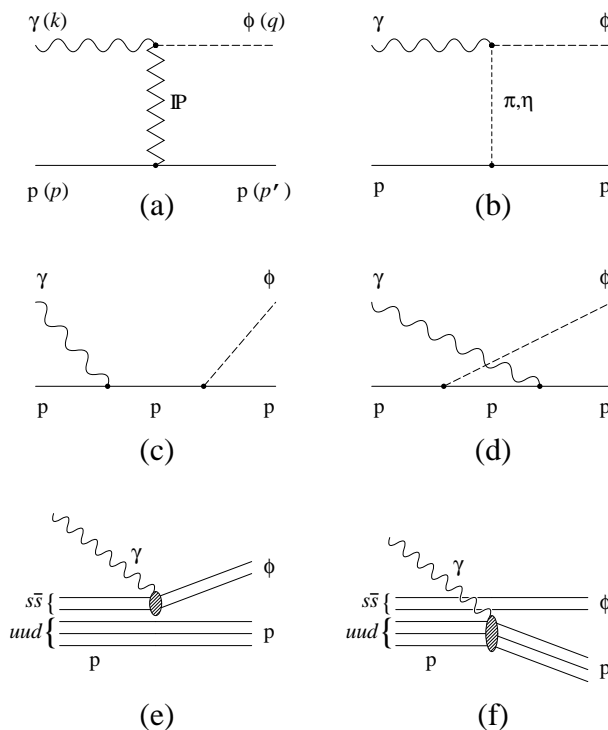


FIG. 1. Diagrammatic representation of ϕ photoproduction mechanisms: (a) Pomeron exchange, (b) (π, η) exchange, (c,d) nucleon pole terms, and (e,f) direct knockout processes.

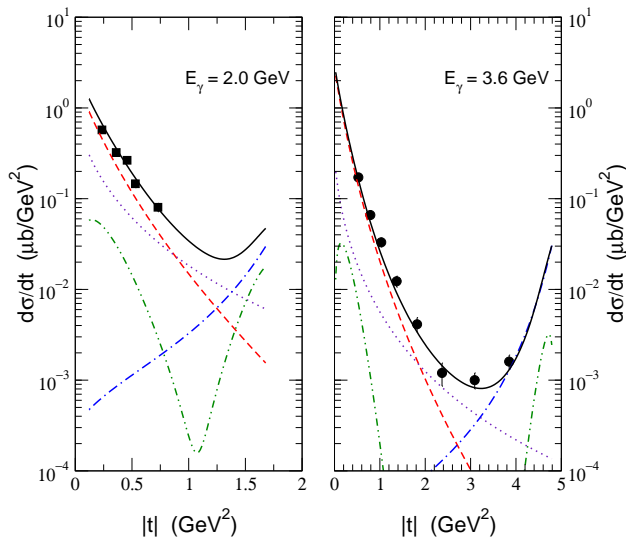


FIG. 2. Differential cross sections of ϕ photoproduction at $E_\gamma = 2.0$ GeV and 3.6 GeV. The results are from Pomeron exchange (dashed), pseudoscalar-meson exchange (dotted), nucleon pole terms with $g_{\phi NN} = -3.0$ (dot-dashed), direct knockouts with $B^2 = 1\%$ (dot-dot-dashed), and the full amplitude (solid). The experimental data are from Ref. [35] (filled squares) and Ref. [19] (filled circles).

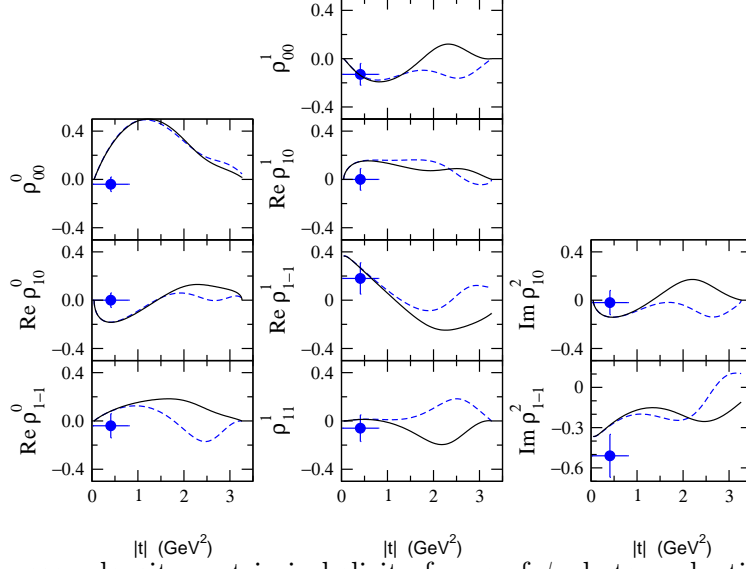


FIG. 3. Vector meson density matrix in helicity frame of ϕ photoproduction at $E_\gamma = 2.8$ GeV with the full amplitude. The solid and dashed lines are obtained with $g_{\phi NN} = -3.0$ and 3.0 , respectively. The data are from Ref. [41] at $E_\gamma = 2.8$ and 4.8 GeV.

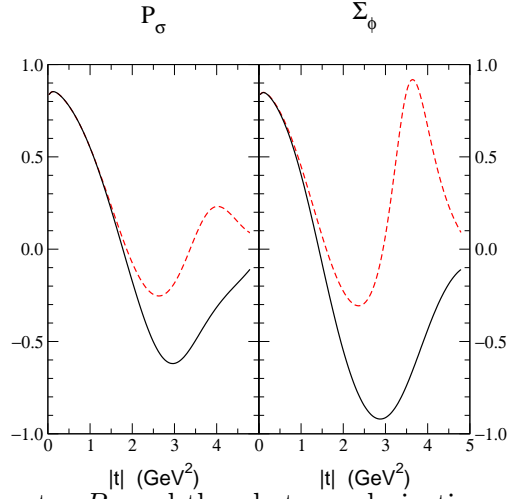


FIG. 4. The parity asymmetry P_σ and the photon polarization asymmetry Σ_ϕ in ϕ photoproduction at $E_\gamma = 3.6$ GeV with the full amplitude. Notations are the same as in Fig. 3.

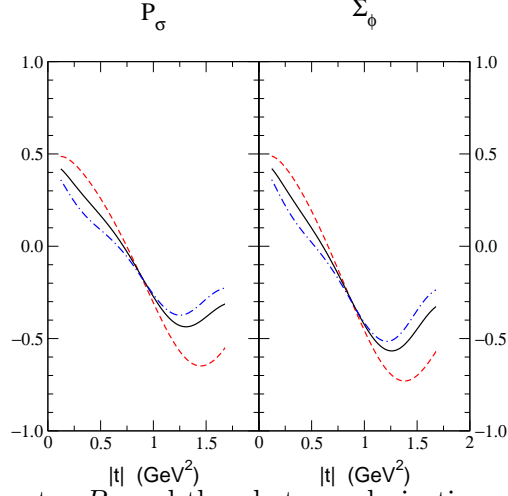


FIG. 5. The parity asymmetry P_σ and the photon polarization asymmetry Σ_ϕ in ϕ photoproduction at $E_\gamma = 2.0$ GeV with the full amplitude with $g_{\phi NN} = -3.0$. The dashed lines are without the knockout mechanisms ($B^2 = 0$). The solid and dot-dashed lines are with $B^2 = 1\%$ and 2% , respectively.